1966

Thermal models for prediction of neutron flux levels in reactors

Larry Dale Schlenker
Iowa State University

THERMAL MODELS FOR PREDICTION OF NEUTRON FLUX LEVELS IN REACTORS

by

Larry Dale Schlenker

A Dissertation Submitted to the
Graduate Faculty in Partial Fulfillment of
The Requirements for the Degree of
DOCTOR OF PHILOSOPHY

Major Subject: Nuclear Engineering

Approved:

Signature was redacted for privacy.

In Charge of Major Work

Signature was redacted for privacy.

Head of Major Department

Signature was redacted for privacy.

Dean of Graduate College

Iowa State University
Of Science and Technology
Ames, Iowa

1966

TABLE OF CONTENTS

I. INTRODUCTION

A. Nature of the Problem

A knowledge of local neutron flux levels is essential for determining the effectiveness of control devices, power density and leakage rates. The influence of geometric and material variables on the flux in a multiplying assembly is implicit in the familiar neutron material balance expression given as:

$$D\nabla^2 \phi - \Sigma a \phi + k\Sigma a \phi = 0 \qquad (1)$$

where one group steady state conditions have been assumed. The first term refers to the attrition of neutrons through leakage while the other terms describe capture loss and fission gain processes. Frequently Equation 1 is rearranged to the Helmhotz form given by 1a.

$$\nabla^2 \phi + \frac{(k-1)\Sigma a}{D} \phi = 0 \qquad (1a)$$

If the reactor is homogeneous or if the intercellular variation of the flux is a heterogeneous reactor can be ignored, Equation 1a can be solved analytically for cases in which the reactor core has a simple geometric figure. Generally, however, both the reactor shape and the pattern of flux control devices introduce complications which are better treated with a digital computer or by similitude techniques using a scale model or analog computer.

The purpose of this study is to investigate the use of temperature profiles to predict neutron flux levels and related phenomena for nuclear

reactors having an arbitrary shape. One group theory is assumed throughout.

B. Advantages of Model Techniques

The selection of a method for solving flux dependent problems having complicated boundary conditions is usually based upon considerations of accuracy and economics. While it is impractical to discuss all methods for the solution of nuclear engineering problems, a few aspects of model methods will be mentioned.

First, the potential for accurate measurement is quite high as demonstrated by the performance of several models discussed below which agree within 1% of the theoretical predictions. In addition, such studies are frequently done with a relatively inexpensive analog of the prototype system.

Models are often constructed so that factors influencing their operation are easily adjusted to give a wide range of performance. This provides a means for selecting the optimum arrangement among the relevant parameters. Also, the experience gained in operating the model will often provide deeper insight into the operation of the prototype.

Finally, a unique feature is that solutions determined by observations performed on a model are determined solely by physical processes within the model. This has the effect of transferring the research responsibility to areas of proper model design and interpretation and eliminates the formal intricacies of direct calculation. This is particularly significant when the shape of the reactor is not easily described

analytically or when the section size of a prototype member is too small for accurate application of diffusion theory.

II. LITERATURE REVIEW

Models may be classified according to various schemes. The present interests are best served, however, by classifying the models according to how the data acquisition measurements are performed, i.e., in either a spacially continuous fashion or at preselected discrete locations in lumped parameter models.

A. Spacially Continuous Models

There have been only a few models proposed of this type all of which use one group analysis. The models appear to be relatively easily constructed and the reported accuracy is very high.

A two dimensional electric model for a reflected heterogeneous reactor of arbitrary cross section is described by Nagao (1). The fuel rods are simulated by constant potential surfaces while resistive films are used to model the moderator and reflector. Voltage measurements are used to predict neutron flux for steady state operation.

Melcher and Murphy (2) have shown that an analogy exists between the neutron flux and the axial component of the electric field intensity when the field is excited as a plane transverse magnetic wave. Studies are made of buckling measurements and the worth of fully extended control rods in center and off center positions for a bare homogeneous reactors having a right cylindrical core. Flux level measurements were predicted with errors of less than 1%.

Temperature profiles in a cooling wax model have been used by Mossop and McGhee (3) to predict flux profiles in a geometrically similar

bare homogeneous prototype. Effectiveness studies were performed for groups of control rods as a parametric function of rod diameter and the degree of insertion.

It might be mentioned that the model discussed in Part II of this paper is also the continuously measurable type. The principal formal reference for the technique of its development is given in "Similitude in Engineering", by Murphy (4).

B. Lumped Parameter Systems

The importance assumed by the analog computer in the solution of nuclear engineering problems is witnessed by the rather large amount of descriptive literature in this field. The selections from the literature used in the following discussion is limited to that which gives an historical outline of the major contributions in developing this tool and indicates the scope of its present application.

Probably the first serious attempt to model diffusion equations with an analog circuit was by Corey, Green and Frederick (5). Description of a reflected one dimensional model is given along with a mathematical development of the circuitry requirements. A simplifying assumption regarding the treatment of reflector parameters was later proposed by Fieno, Schneider and Spooner (6).

Honeck and Ott (7) then built a two group system consisting of a two dimensional 800 element array. Space dependent flux profile problems were solved by assuming an initial thermal neutron flux distribution and iterating a set of voltages corresponding to the thermal and fast neutron flux distributions throughout the network.

Other significant investigations were carried on by Liebmann (8) who studied flux profiles around cavities in reflected reactors by means of a simulated one group treatment. The method was extended to a two group treatment and published posthumously, (9). Differences between these tests and analytic solutions were also less than 1%.

Suggestions for shortening the tedious iterative process by which the voltage pattern is adjusted in the circuit network have been made by Eaton and Long (10). Their simplified approach has been successfully tested at Purdue University.

At about this point in its development, the analog computer gained widespread acceptance in the nuclear engineering industry. As early as 1957 a survey article (11) lists the active use of 14 analog computers by government and industrial groups engaged in nuclear research. The range of problems being solved appeared to remain primarily concerned with core design and associated problems of reactor physics. Typical examples are studies of multi-region reactors by Bayly and Pearce (12) and reactor kinetics problems by Kelber, Just and Morehouse (13), though occasionally unusual items occur such as an analog model of an entire reactor power plant by George and Sesonske (14).

As in the case of many engineering disciplines, the modern analog computer had its roots in early mathematical discussions of pure science. It was observed that the equations for the diffusion of neutrons in a moderating media and the flow of current in an electric line are similar. The partial differential equations were then replaced by finite difference

equations and these, in turn were simulated by "lumped" electrical parameters. This development is outlined in references 5, 7, 8, and 9.

III. PART I-FEASIBILITY INVESTIGATION FOR THE USE OF THERMAL SETTING EPOXY RESIN FOR PREDICTION OF NEUTRON FLUX PROFILES IN A BARE HOMOGENEOUS REACTOR

A. Objective

The use of liquid fuel homogeneous reactors has been studied extensively (15, for example). Often the shape of the reactor core is irregular to accomodate control devices or maintain liquid flow patterns which enhance a uniform slurry density. Since the predictions of neutron flux profiles is not easily achieved in irregular shapes by standard analytic procedures, a simple technique giving accurate results would be of value.

The purpose of this study is to investigate the feasibility of using temperature in a geometrically similar thermal setting epoxy casting to predict one group neutron flux profiles in a bare homogeneous reactor with an arbitrary shape.

Determining the criteria for judging "feasibility" is, of course, somewhat subjective. What has been adopted is the following.

1. The system just demonstrate the ability to predict the thermal flux distribution in a sphere, as a selected shape.
2. It must indicate a capability for modeling a general shape. The test for the latter is to compare the temperature profiles in cylindrical model in the direction of its plane and curved surfaces. If the results of a particular model, say a right cylinder, are similar for regions bounded by plane and curved

B. Dimensional Analysis Assumptions and Approach

The time-temperature history of a typical thermal setting epoxy resin is qualitatively shown by the dark line in Figure 1.

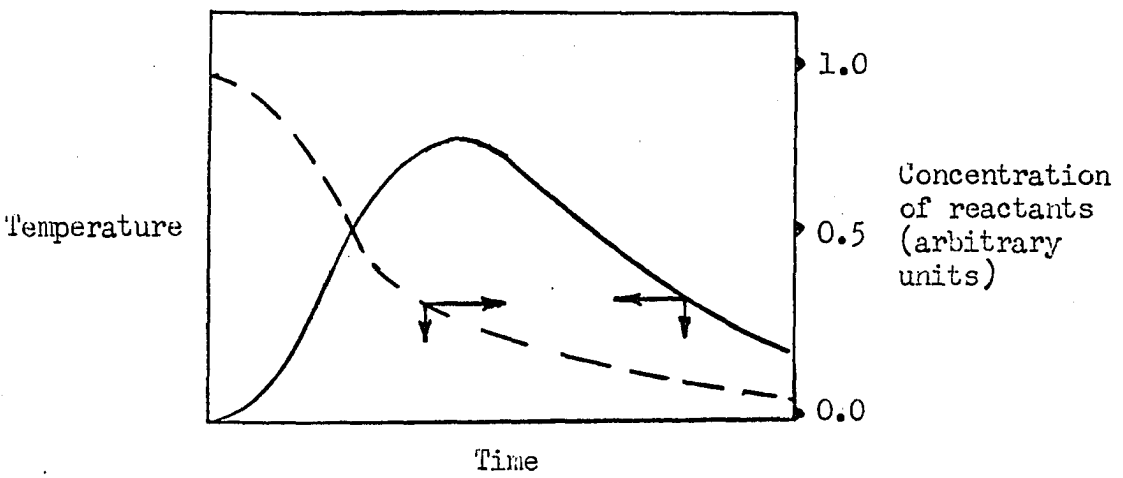

Figure 1. Typical relationships for epoxy resins

The reaction progresses according to Arrhenius' Law i.e., exponentially increasing with temperature and concentration. The thermal excursion of the reaction is limited, however, by the finite quantity of reactants which ultimately achieve dynamic equilibrium with the products of reaction in the thermal setting process.

A thermodynamic balance for a unit volume of exothermic material is given as follows:

$$\frac{\partial \theta}{\partial t} = \frac{K}{\rho c} \nabla^2 \theta + \frac{H_1 r}{\rho c}$$

where

θ = Temperature

t = Time

K = Thermal conductivity

ρ = Mass density

c = Specific heat

H_1 = $\dfrac{\text{Heat}}{\text{Moles of product which appear by reaction}}$

r = $\dfrac{\text{Moles of product which appear by reaction}}{(\text{unit volume})(\text{unit time})}$

The term "r" is called the reaction rate which depends upon the temperature and concentration of the reactant. If the concentration of the reactants is denoted $C_o\ (\theta_i, t, x)$ where θ_i denotes initial temperature, t denotes running time and x accounts for all geometric variables, r will have the approximate form predicted by Arrhenius' Law, namely:

$$r = C_o\ (\theta_i, t, x)\ k_o e^{-E/R\theta}$$

where

k_o = Frequency factor

E = Activation energy

R = Boltzmann constant (per mole basis)

θ = Absolute temperature

Even though the above equation for the reaction rate is given in a somewhat idealized form, it is apparent by its form that r cannot in general be reasonably approximated by a linear function of θ and, therefore, the analysis cannot proceed by making a direct comparison of the thermodynamic balance expression and Equation 1a.

Other means of analysis are available. In forming epoxy castings it has been qualitatively observed that the central regions become the

hottest. This suggests that details of the setting mechanism are sensitive to certain aspects of the casting geometry. Experience has also shown that the chemical and physical properties of the material and the temperature of the casting environment affect the local maximum temperature in the casting. These somewhat vague ideas serve to indicate the existence of a parametric relation between temperature and position in the epoxy model which hopefully may be formalized and quantitatively explored by dimensional analysis. Toward this end, the following list of variables was selected for analyzing spheres of various sizes.

Table 1. Sphere variables

Variable	Dimension	Quantity
r	L	Position
R	L	Radius
θ_1	θ	Max. Temp., Center Position
θ_2	θ	Max. Temp., Arbit. Position
θ_3	θ	Max. Temp., Boundary
θ_4	θ	Mix Temp.
θ_5	θ	Bath Temp.
T_1	T	Mixing Time
T_2	T	Pouring Time
K	$H L^{-1} T^{-1} \theta^{-1}$	Thermal Conductivity
ρ	ML^{-3}	Density
c	$HM^{-1}\theta^{-1}$	Specific Heat

Since the variables are initially selected by somewhat informal processes, with the excepted restriction that each dimension must appear in at least two variables, the overall success of the analysis depends in part upon an astute selection. Tests must be performed to evaluate the latter.

There are twelve variables in five dimensions requiring seven independent pi terms. H is treated as an independent variable because no work is done by the system. This procedure is described on page 193 of reference 4. The pi terms are given in Table 2 and discussed in the next two sections.

Table 2. Pi terms for spheres

1.	$\frac{r}{R}$
2.	$\frac{\theta_2 - \theta_3}{\theta_3}$
3.	$\frac{\theta_1 - \theta_3}{\theta_3}$
4.	$\frac{\theta_3}{\theta_4}$
5.	$\frac{\theta_4}{\theta_5}$
6.	$\frac{T_1}{T_2}$
7.	$\frac{KT_1}{\rho c R^2}$

A similar approach has been used for the analysis of cylinders. The selection of variables and pi terms for cylinders is given in Tables 3 and 4.

Table 3. Cylinder variables

Variable	Dimension	Quantity
r	L	Radial position
h	L	Axial position from center
R	L	Radius
H	L	Height
θ_1	θ	Max. temp., center position
θ_2	θ	Max. temp., arbit. position
θ_3	θ	Max. temp., boundary
θ_4	θ	Mix temp.
θ_5	θ	Bath temp.
T_1	T	Mixing time
T_2	T	Pouring time
K	$H\ L^{-1}\ T^{-1}\ \theta^{-1}$	Thermal conductivity
ρ	$M\ L^{-3}$	Density
c	$H\ M^{-1}\ \theta^{-1}$	Specific heat

Table 4. Pi terms for cylinders

1.	$\frac{r}{R}$
2.	$\frac{\theta_2 - \theta_3}{\theta_3}$
3.	$\frac{\theta_1 - \theta_3}{\theta_3}$
4.	$\frac{2h}{H}$
5.	$\frac{\theta_3}{\theta_4}$
6.	$\frac{\theta_4}{\theta_5}$
7.	$\frac{R}{H}$
8.	$\frac{T_1}{T_2}$
9.	$\frac{KT_1}{\rho cRH}$

The procedure is to plot ordinate values of the quotient of the local maximum temperature rise divided by the central maximum temperature rise versus abscissa values of the fractional distance of a point measured along a line projecting from the center of the model to the boundary. Plots of these analyses are given in "Results".

C. Test Apparatus and Procedure

The approach in all cases was to build the molds with iron constantan thermocouples rigidly positioned in preselected locations. Epoxy was then poured into the mold cavity through a hole which was later taped shut. Following the suggestion of using an isothermal environment to establish the thermal analog of a vacuum surrounding a prototype (16, p. 113), the models were immersed in a circulating water bath throughout the test. The maximum thermocouple millivolt readings were observed during the ensuing exothermic reaction with a model 2745 Honeywell potentiometer and recorded.

The pi terms have been selected and arranged in Graphs 1, 2, and 3 so that the abscissa values are the quotient of the local maximum temperature rise divided by that at the center of the model and the ordinate values are the fractional distance from the center of the mold to the bounding surface. In each case, however, a third pi term which depends upon the size of the model was allowed to vary, i.e., π_7 for the spheres and π_9 for the cylinders. As might be expected, model size influences the shape of curves. In addition, the rerun with spheres of size 2 using the second epoxy shipment (see Table 6) indicates that the chemical composition of the epoxy to generate heat also influences the curve shape.

It might be mentioned that the data at $\pi_1 = 0.75$ (and $\pi_4 = 0.75$) were most subject to scatter. This is discussed in "Part I Error Analysis", Appendix B, and reflects the method of data reduction as well as physical reasons.

Details of the molds are shown in Figures 2 and 3. All spherical containers were made of plastic while the cylindrical containers were metal. To avoid a bias in surface temperatures due to variable thermal conduction properties of the walls of the molds, a small metal clip was attached to the outermost thermocouples and these, in turn, positioned at the inside wall surfaces.

Table 5. Model dimensions

Model Number		Inside radius cm	Inside Height cm
Spheres	1	2.59	----
	2	3.51	----
	3	4.10	----
Cylinders	4	3.16	5.28
	5	3.61	6.66

The epoxy, 3M SK-680[a], was filled with Dixon's number 1 flake graphite[b] at the weight ratio of 1 part graphite to 10 parts epoxy to increase the thermal conductivity of the casting. The graphite enhances the cooling effect of the water bath and hence permits the use of larger models for a given temperature excursion. In all cases the water bath was maintained at a temperature of 15 ± 1° C and the epoxy mixture was 20 ± 1° C prior to mixing. The mixing times were

[a]Minnesota Mining and Manufacturing Company, St. Paul, Minnesota.

[b]The Joseph Dixon Crucible Company, Jersey City, New Jersey.

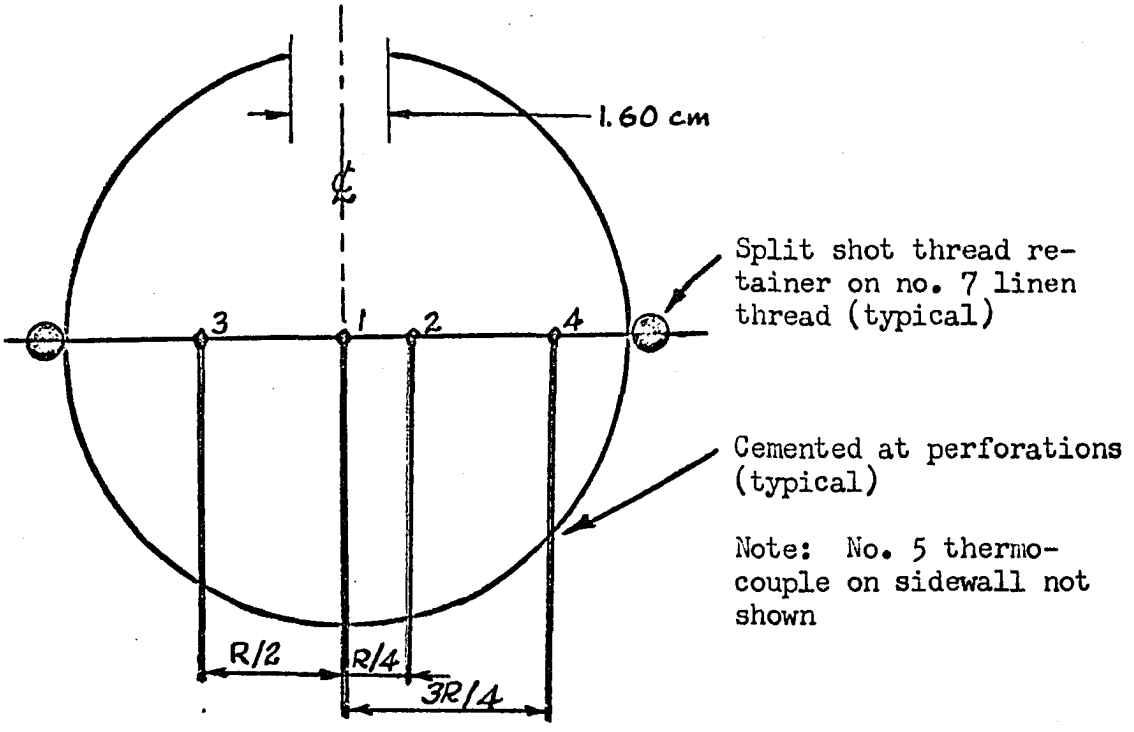

Figure 2. Thermocouple positions in spherical molds

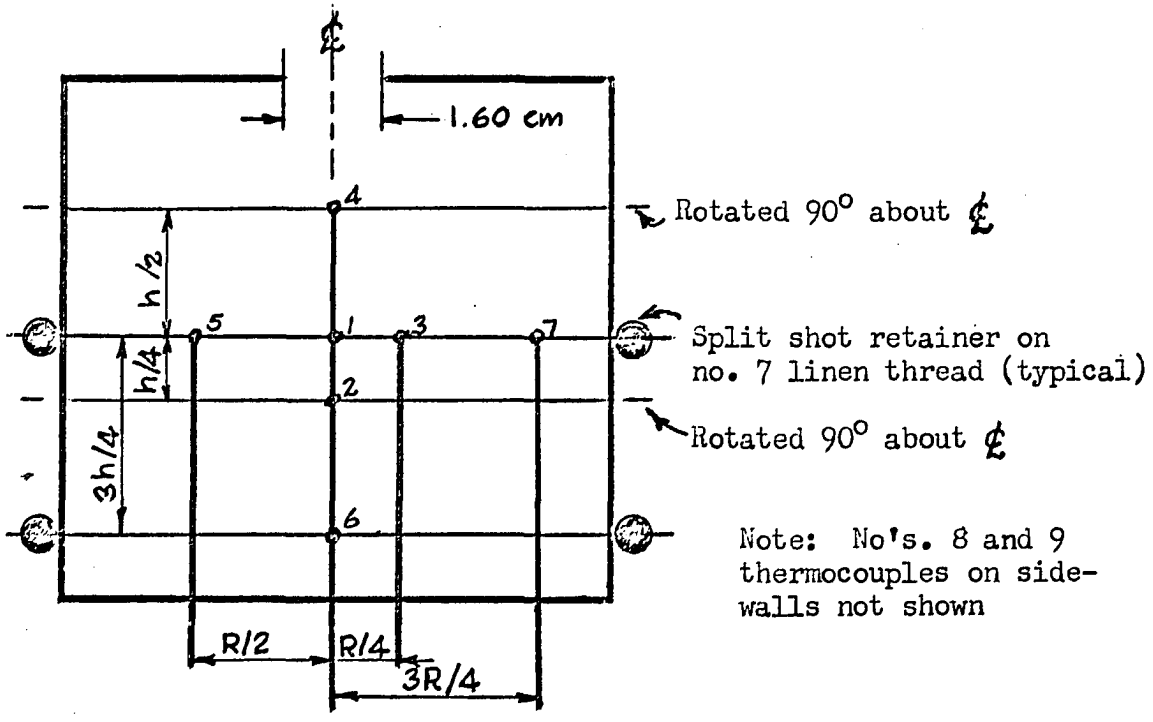

Figure 3. Thermocouple positions in cylindrical molds

held constant at 90 seconds and the pouring times vary close to 60 seconds. This results in π_4, π_5, and π_6 being constant and π_7 = constant/R^2 for the spheres and π_5, π_6, π_7, and π_8 being constant and π_9 = constant/RH for the cylinders.

The maximum temperature excursion occurred about 15 minutes after pouring. This occurs first in the central region and it was observed to occur a few seconds later at points located progressively toward the bounding surface.

Two shipments of presumably identical epoxy were used during the tests. The spheres were tested with the first shipment and the cylinders were tested with the second shipment. The second shipment gave larger temperature excursions (see Appendix A, Part I Data) which may have been due to evaporation losses of an aromatic constituent during handling of the first shipment. The results are shown and discussed in the next section.

D. Results

Graph 1 shows that the theoretical curve is closely matched by the size 1 spheres. All these data have ordinate errors of less that 0.03 when compared with the theoretical distribution given by $\sin\frac{\pi r}{R} / \frac{\pi r}{R}$. Even though the epoxy spheres do not match the design conditions necessary for serving as true models of the homogeneous spherical reactor core, it is encouraging to note that for a particular sphere, in this case the smallest sphere, there is good agreement between the temperature profile and the theoretical flux profile for the same geometry.

Graphs 2 and 3 show the superposition of radial and axial temperature

distributions for cylinders of two sizes. The cylinders were arbitrarily proportioned with a height to radius ratio of 1.845. It is clear from the graph that size again influences the curve shape. The important feature is, however, that the radial and axial data lie near a single curve and are particularly close in the central regions of the casting. This indicates that the analysis technique can be used to predict flux level variations arising from considerations of boundary curvature, which is to say, a general shape. This seems especially true when the so-called "general shape" is a minor variation of a sphere or cylinder, a likely situation.

The question of generating reproducible data cannot be resolved here in a yes or no fashion. Examining the data, (Appendix A), it is found that 77% of the values agree within 5% of the average value for all given points, and it is likely that ammending the technique, as discussed in "Recommendations", would improve this figure. The difficulty in making an evaluation stems in part from not knowing the requirements of all situations in which it might be applied and, additionally, that the scheme of testing may itself be a source of error as well as the epoxy mechanism per se. If a value judgment may be offered, the accuracy seems at least reasonable and may be improved.

A complete evaluation of the results must also, however, consider other research. In this case, the only competing method for predicting a continuously measurable flux distribution in a bare homogeneous reactor of arbitrary shape is that of the cooling wax model described in reference 3.

The cooling wax method has the advantage of being developed in a usable form whereas the epoxy model concept is not. While there are differences in testing techniques involved, the relative effort required is probably not significant. The most definitive consideration may be accuracy where again, the epoxy model cannot be presently evaluated in terms of ultimate potential.

Some data suggest, however, that the epoxy method is relatively stable and therefore reproducible. When attempts were made to intentionally introduce errors (see Appendix A) by poor mixing and distortion of the thermocouple bead size, the resulting errors were less than one percent. The scatter in the data is generally greater than this, though, suggesting a bias is introduced in the testing technique.

The wax analog method also appears to be somewhat variable. Figures 6 and 7 of the cited reference do not indicate symmetric temperature profiles for measurements taken in a geometrically symmetric model It would seem, then, that no clear choice is presented at present.

E. Recommendations for Development Study

In the event of a continued investigation, the following four items are recommended for consideration.

First, the 90-second mixing time was found to increase the volume 6% by entraining air into the mixture. This would then result in a bubble forming on the interior surface. Probably a gentler stirring action could prevent this.

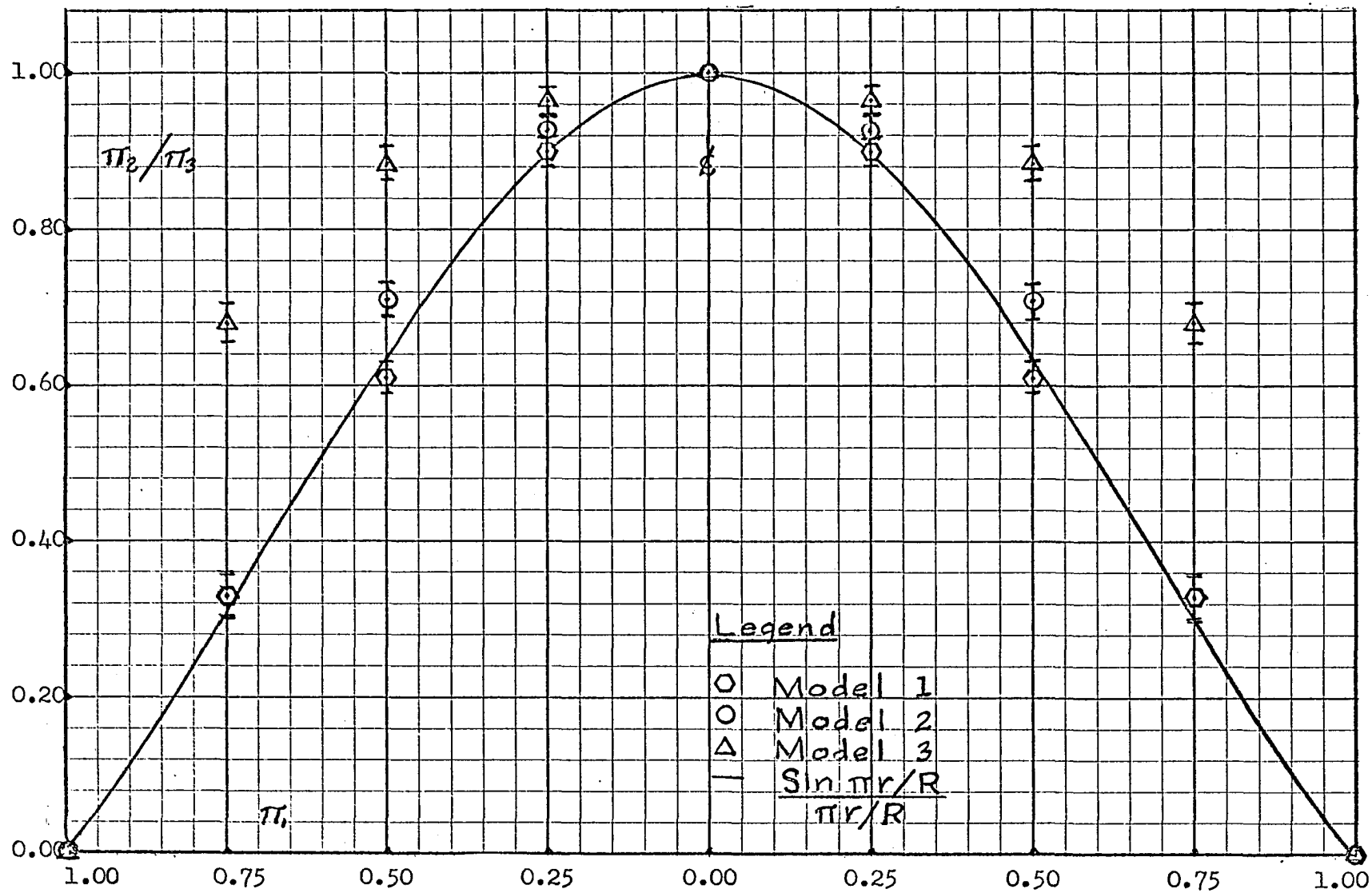

Graph 1. Radial direction thermal excursions for spheres

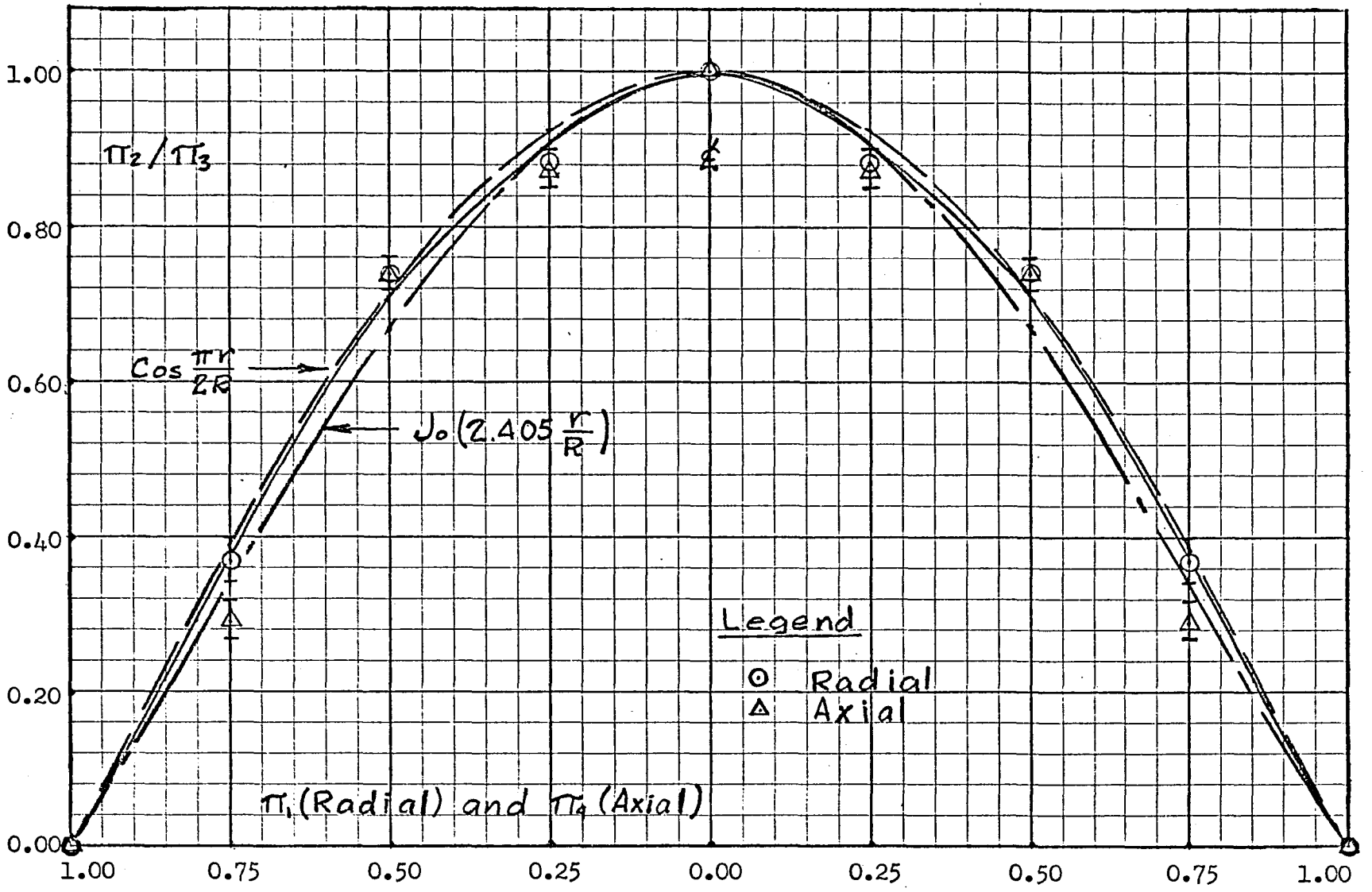

Graph 2. Superposition of radial and axial direction thermal excursions for cylinder no. 4

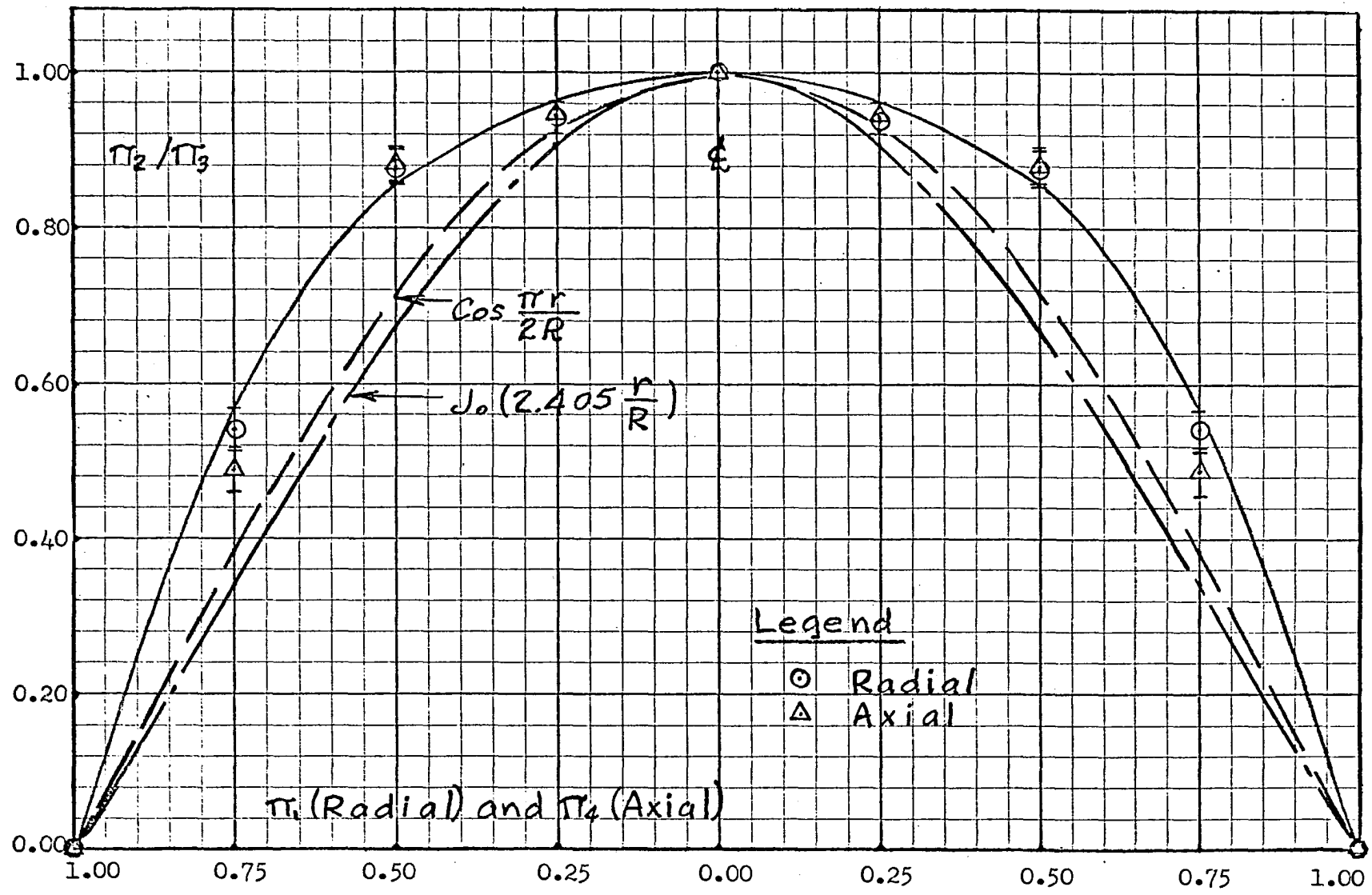

Graph 3. Superposition of radial and axial direction thermal excursions for cylinder no. 5

Table 6. Average relative thermal excursion in spheres

Values of π_2/π_3 in model size	π_1 values				
	0.00	0.25	0.50	0.75	1.00
1	1.000	0.898	0.611	0.329	0.000
2	1.000	0.924	0.707	0.329	0.000
3	1.000	0.966	0.884	0.681	0.000
$\frac{\sin \pi r/R}{\pi r/R}$	1.000	0.900	0.637	0.300	0.000
2 (2nd Epoxy shipment not plotted)	1.000	0.946	0.826	0.443	0.000

Table 7. Average relative thermal excursion in cylinders

Values of π_2/π_3 in model size	π_1 (radial) and π_4 (axial) values				
	0.00	0.25	0.50	0.75	1.00
4 (radial)	1.000	0.942	0.874	0.542	0.000
4 (axial)	1.000	0.947	0.879	0.488	0.000
5 (radial)	1.000	0.884	0.738	0.371	0.000
5 (axial)	1.000	0.868	0.741	0.291	0.000

Second, a stable, long shelf life epoxy is desirable. Preferably it would not contain amines or other fillers which tend to evaporate and thus change the constitution of the residual material.

Third, it was noticed that the time rate of temperature change was greatest in the central regions of the model. This might be a valuable variable to consider if a chart recorder is available.

IV. PART II-THERMAL ELECTRIC MODEL OF A REFLECTED HETEROGENEOUS REACTOR

A. Objective

Experimental research with heterogeneous reactors is largely concerned with prototype studies and the operation of analog systems. Both methods involve considerable expense and often the analog systems are only two dimensional. Unfortunately, the only continuously variable model of a heterogeneous reactor (1) is also two dimensional.

The purpose of this section is to develop the theoretical basis for a continuously measurable one group model of a three dimensional reflected heterogeneous reactor. An arbitrary shape and the use of unsymmetrically located partially inserted control rods will also be allowed.

B. Basis of Analogy and Modelling Assumptions

As in Part I, the scheme again is to use temperature in the model as the analog of neutron flux in the prototype. The following assumptions are made for the reactor:

1. All neutrons have the same energy.
2. The reactor consists of fuel, moderator, reflector and control devices.
3. All neutron captures occur in the fuel and control rods.

The basis of the analogy consists of showing that the equation which describes the temperature in the model has the same form as that for

the nuclear reactor, i.e., Equation 1a. Because the physics of operation in a heterogeneous reactor must vary from one region to another, however, the general Equation 1a will assume particular values in each region. Specifically, the nuclear constants must characterize the material of each region and also assumption number three requires that only diffusion processes occur in the moderator and reflector.

Similarly, then, the general equation describing the thermal model must assume the particular form of Equation 1a in all homologous locations. This is to say there must be heat sources in the model which correspond to neutron sources in the fuel rods of the prototype and source free thermal diffusion processes in the model regions which correspond to the moderator and reflector.

It will be noticed that the usual assumptions that the moderator serves as a source of thermal neutrons and the fuel rods act as a sink are inverted. The result is that the proposed model is restricted to predicting phenomena in which details of flux variations within individual cells are not of concern.

Since Equation 1a is a statement of neutron density equilibrium for the prototype, a possible starting point in deriving the model characteristic equation is the condition of thermal equilibrium in the model given by:

$$\text{Heat sources} - \text{Heat sinks} - \text{Heat leakage} = 0 \qquad (2)$$

Assuming a per unit volume basis of calculation, the familiar thermal diffusion equation describes the leakage.

$$-\frac{K}{\rho c}\nabla^2\theta = -\frac{\partial\theta}{\partial t} \qquad (3)$$

or

$$-K\nabla^2\theta = -\frac{\partial Q}{\partial t} \qquad (3a)$$

where

$$dQ = \rho c\, d\theta$$

The form of Equation 1a further suggests that the thermal sources and sinks must be linear functions of temperature. It will be seen that this requires a specific type of heating material. For now, however, the form of the equation is the principal interest so that

$$\text{Source} = A\theta = \frac{\partial Q}{\partial t} \qquad (4)$$

$$\text{Sink} = B\theta = -\frac{\partial Q}{\partial t} \qquad (5)$$

where θ = temperature

ρ = density

K = thermal conductivity

c = specific heat

Q = heat/unit volume

t = time

A, B = dimensional constants

Substituting Equations 3a, 4 and 5 into Equation 2 gives:

$$A\theta - B\theta + K\nabla^2\theta = \left(\frac{\partial Q}{\partial t}\right)_{net} = 0 \qquad (6)$$

for steady state operation.

Rearranging:

$$\nabla^2 \theta + \frac{S}{K} \theta = 0 \qquad (7)$$

where $S = (A - B)$ is the net thermal source constant. It will be noticed that Equation 7 for the model has the same form as 1a for the prototype.

As a convenience, the symbols used in this section are identified in Appendix C along with a dimensional review of selected terms and equations.

It has been assumed that the thermal sources are electrically powered and linear in temperature. One possibility is to use resistance heating between two conductors which are maintained at a constant voltage, E, along the length of the model fuel element. This gives

$$\text{Electric power} = \frac{E^2}{R} = C_1 \theta \qquad (8)$$

where C_1 is a constant. This implies that the resistance, R, is inversely related to temperature. Such a material is said to have a negative coefficient of resistivity. Though the specific temperature-resistivity relationship may vary among materials, the requirement is that R and θ vary over the temperature range of operation in a hyperbolic fashion. Several resistive materials display this property, notably the element carbon (17, p. 2193) and sintered metallic oxides of cobalt, copper, iron, nickel and uranium (18).

The zero of temperature, θ_0, for the model temperature scale corresponds to the location where the electrical resistance approaches

infinity. This shown schematically in Graph 4. Widespread commercial application of materials having this characteristic is found in various forms of thermistors.

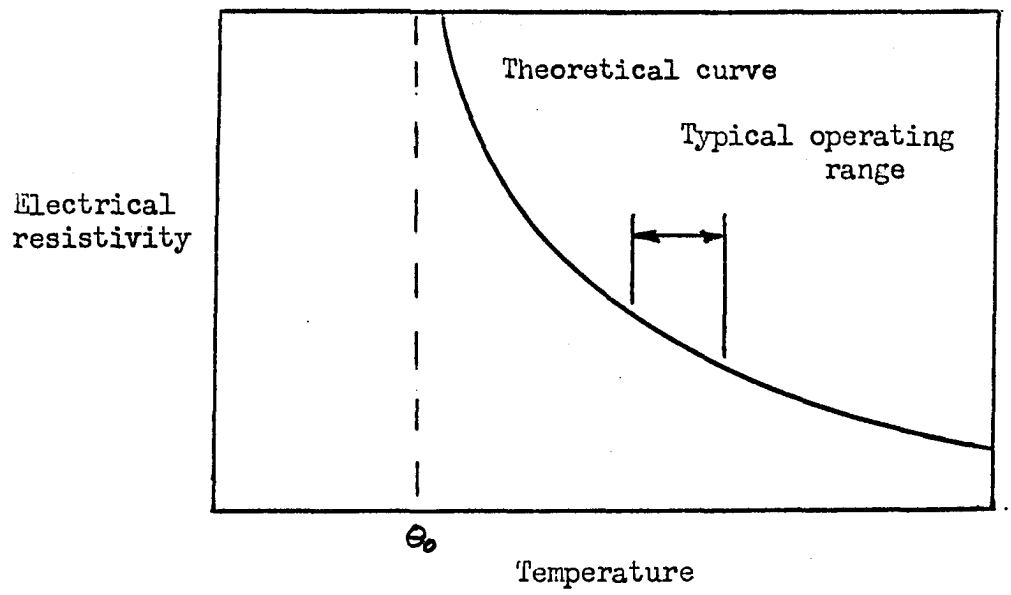

Graph 4. Schematic of resistivity-temperature relationship

The specific power generation can then be designed to accommodate a range of values by adjusting the width of resistive material between parallel conductors. Other geometries are possible, of course.

C. Development of Prediction and Design Equations

When the characteristic equations for the prototype and model have the same form, a model design may be established directly by equating corresponding coefficients. Somewhat more latitude is permitted in the design of the model, however, by introducing dimensional constants

into the prediction and design equations through the indirect modelling procedure. This approach is used in the following development.

As a convenience, the characteristic equations for each region are listed in Table 8.

Table 8. Characteristic equations

Region	Prototype	Model
Fuel	$\nabla^2\phi + \frac{(k-1)\Sigma a}{D_f}\phi = 0$	$\nabla^2\theta + \frac{S}{K_f}\theta = 0$
Moderator	$\nabla^2\phi = 0$	$\nabla^2\theta = 0$
Reflector	$\nabla^2\phi = 0$	$\nabla^2\theta = 0$

Subscripts of f, m, and r shall refer to fuel, moderator and reflector respectively.

In addition to the above equations, two boundary conditions are important. First, it is recalled that the temperature θ_0 in the model corresponds to a zero neutron flux. This means that "black" control devices and the non-reflecting reactor environment correspond to a temperature of θ_0 in the model. Secondly, the neutron currents are equal on each side of the fuel-moderator and moderator-reflector interfaces. These conditions will be used later.

It is assumed that the prediction equation has the form

$$\phi = n_1 \theta$$

where n_1 is a dimensional constant. Related information is given in

Appendix C. This is also seen to be a generalization of the first boundary condition.

The model is further assumed to be a scale reproduction of the prototype, i.e., geometrically similar. Therefore, the first design equation is

$$(1)\quad L = n_2 L_A$$

with the subscript A referring to model analog.

The prediction equation and first design equation may now be substituted into the prototype fuel region characteristic equation giving

$$\left(\frac{\partial^2}{\partial(n_2 x_A)^2} + \frac{\partial^2}{\partial(n_2 y_A)^2} + \frac{\partial^2}{\partial(n_2 z_A)^2}\right) n_1 \theta + \frac{(k-1)\Sigma a}{D_f} n_1 \theta = 0 \quad (9)$$

or

$$\frac{n_1}{n_2^2}\nabla^2 \theta + n_1 \frac{(k-1)\Sigma a}{D_f} \theta = 0 \quad (9a)$$

which is rearranged to

$$\nabla^2 \theta + n_2^2 \frac{(k-1)\Sigma a}{D_f} \theta = 0 \quad (9b)$$

Equating the coefficient of the linear term in 9b to that of the model characteristic equation for the fuel region established the design condition for the heat generation in the model fuel rods, i.e.,

$$(2)\quad \frac{S}{K_f} = n_2^2 \frac{(k-1)\Sigma a}{D_f}$$

The third and fourth design equations are derived from the second boundary condition. For simplicity consider a plane interface separating two regions, say fuel and moderator regions. The neutron current is related to the diffusion coefficient and flux by

$$J = - D\nabla\phi \tag{10}$$

and applying the boundary conditions gives

$$- J = D_f \frac{\partial \phi_f}{\partial L} = D_m \frac{\partial \phi_m}{\partial L} \tag{11}$$

but

$$\phi = n_1 \theta$$

and

$$L = n_2 L_A$$

so that

$$D_f \frac{n_1}{n_2} \left[\left(\frac{\partial \theta}{\partial L}\right)_f\right]_A = D_m \frac{n_1}{n_2} \left[\left(\frac{\partial \theta}{\partial L}\right)_m\right]_A \tag{12}$$

or simply

$$D_f \left[\left(\frac{\partial \theta}{\partial L}\right)_f\right]_A = D_m \left[\left(\frac{\partial \theta}{\partial L}\right)_m\right]_A \tag{12a}$$

Now considering the Coulomb heat conduction equation

$$H = K A t \left(\frac{\partial \theta}{\partial L}\right) \tag{13}$$

where

H = heat

K = thermal conductivity

A = area normal to the thermal gradient

t = time

$\frac{\partial \theta}{\partial L}$ = thermal gradient

A rearrangement gives

$$\frac{\partial \theta}{\partial L} = \frac{H}{K A t} \tag{13a}$$

But it is observed that specific heat transfer rate $\frac{H}{tA}$ must be equal on each side of the homologous model interface so that

$$\frac{\partial \theta}{\partial L} = \frac{C_2}{K} \tag{14}$$

where C_2 is a proportionality constant.

Substituting Equation 14 into Equation 12a gives design equation 3:

$$(3) \quad \frac{D_f}{D_m} = \left(\frac{K_f}{K_m} \right)_A$$

Similar considerations at the moderator reflector interface give design Equation 4:

$$(4) \quad \frac{D_m}{D_r} = \left(\frac{K_m}{K_r} \right)_A$$

A physical interpretation of the significance of D and K in influencing the neutron flux and temperature profiles in their respective systems is suggested by recognizing that axial diffusion within a region near an interface will influence an adjacent region as well as would radial transport across the interface. Therefore it would be anticipated

that some regulatory statements are required to insure proper modelling of the augmenting transport modes.

For convenience, the results of this section are collected and recapitulated.

Prediction Equation:

$$\phi = n_1 \theta$$

Design Equations:

$$(1) \quad L = n_2 L_A$$

$$(2) \quad \frac{(k-1)\Sigma_a}{D_f} n_2^2 = \frac{S}{K_f}$$

$$(3) \quad \frac{D_f}{D_m} = \left(\frac{K_f}{K_m} \right)_A$$

$$(4) \quad \frac{D_m}{D_r} = \left(\frac{K_m}{K_r} \right)_A$$

D. Operational Feasibility

A model cannot be developed unless there are materials available which satisfy design Equations 2, 3, and 4. In this section a set of nuclear parameters have been assumed for examination of the requirements subsequently placed upon the thermal conductivity and specific heat generation rate in the model.

Table 9 lists a set of reasonable nuclear parameters.

Table 9. Nuclear constants

Nuclear constant	Value	Source
k-1	0.20	Estimated
Σ a (Nat. Uran.)	0.367 cm^{-1}	Reference 19
D_f (Nat. Uran.)	0.710 cm	Reference 19
D_m Graphite	0.917 cm	Reference 20
D_r Graphite	0.917 cm	Reference 20

Assuming the length scale n_2 is 10 and substituting:

$$\frac{(k-1)\Sigma_a}{D_f} n_2^2 = \frac{(0.20)(0.367)}{(0.710)} 100 = 10.3 \text{ cm}^{-2}$$

At this point several alternatives are possible. The most direct is to search for a material or, more likely, a set of fabricated materials whose S/K quotient is 10.3 cm^{-2}. It may be desirable, however, to model both the fuel and coolant using weighted nuclear coefficients which characterize the gross fuel-coolant region. In this event and using sodium as the coolant, preliminary calculations show the S/K quotient is about ten times smaller. Two ideas emerge, namely that requirements on S/K vary considerably with the modelling assumptions and secondly, that in order to achieve specific values of S/K it is likely that a composite material would be required. It is not too meaningful to carry this calculation further because of the wide range of possibilities, however, there is one additional important feature related to this design equation. That is there is no requirement upon the actual level of power dissipation.

The units of S are gm cal/cm^3 θ^o sec., but the temperature (which varies with location, of course) of the model is not specified. What this means is the relative temperature distribution in the model temperature scale will always be the same though the actual average temperature might be adjusted by changing the electric driving voltage. The analogous situation occurs in a reactor where adjusting the power output will change the average flux level but not the relative flux distribution. This is a fortunate situation because, as a consequence, the model can be operated at an arbitrarily low power level and avoid the potentially unstable operation in which a hot fuel zone whould generate still more heat faster.

Design equations 3 and 4 merely require that the ratio of thermal conductivity constants for any given regions in the model must be the same as the ratio of neutron diffusivity constants for the homologous regions in the prototype.

Since the ratio of D's in the above example are only about 4:1 it would appear that these requirements can be easily met. In fact, the moderator and reflector, being passive elements, have only the design requirements of geometric similarity plus the proper thermal conductivity values which suggests that they may be particularly easy to construct.

The selection of materials in a development project may also be subject to other considerations, such as the method and ease of temperature measurements.

E. Applications

1. The study of flux profiles near control devices

A thermal-electric model should be suited to the study of reactor control analysis. Geometric similarity requires that all channels provided for the insertion of control rods be reproduced to scale in the model. Black neutron absorbers may then be simulated by similarly scaled members which are maintained at θ_0 with circulated coolant or other means. The isothermal envelops which are developed in the control region will then predict the flux contours in the prototype.

There are two important advantages of this model. First, exact geometric similarity makes no compromising assumption that the void created by a partially withdrawn control rod is filled with core material.

Secondly, the effects of control rods having cross sectional dimensions less than two or three mean free paths may be studied using a model whereas analytic approaches using diffusion theory are not reliable for this case.

2. Determination of optimum fuel arrangement for a continuous mixing cycle

The position of fuel rods are often changed at various stages of burnup to flatten the flux profile or effect a higher fractional burnup. It appears that a particularly easy method to determine the optimum available patterns is feasible.

Let us assume the model fuel rods are segmented in relatively short lengths and mechanically detailed to preserve the electric potential integrity along the total length of each fuel rod emplacement. It is

further required that the strength of the source term S/K be scaled to steps in the articulated segments over a range of values corresponding to the range of $\frac{(k-1)\Sigma a}{D}$ values of the fuel rods. They can then be inserted in the model core where they all are driven by the same electric potential, E.

It is essential, however, that particular patterns of the graded fuel segments be established. The requirement is that the number of rods being "burned out" of a particular source strength $(S/K)_j$ must equal the number entering that stage from a slightly "enriched" state $(S/K)_{j-1}$. This is necessary to avoid the condition in which an excess or shortage of fuel elements having a particular enrichment would develop in the normally cycled operation of the prototype.

The optimum nuclear power arrangement is simply predicted. Observing that the corresponding thermal flux developed in the model is directly related to the electrical power supplied, merely introducing an ammeter in the feeder lines will indicate the relative power of each arrangement. Individual cells could be monitored in this manner as well.

Of course each of these procedures is an iterative process and a little searching would be required to optimize the arrangement. In addition, it is required that thermal equilibrium be established before comparative measurements are taken.

F. Conclusions and Recommendations

The proposed thermal-electric model combines a set of desirable features which are unique among reactor simulation systems. It is the

first spacially continuous three dimensional model of a heterogeneous reactor. In addition the modelling technique can accommodate a reflector, control devices, and a reactor core or individual members of arbitrary shape.

The areas of application described in this thesis include reactor control and various fuel burnup rate problems. It is recommended, however, that two additional areas be studied. These are the extension of the present model to predict unsteady state operation and secondly, to investigate the possibility of extending the thermal-electric model concept to include two group analyses.

V. LITERATURE CITED

1. Nagao, Shigeo. Electrical analogy solves nuclear design problems. Nucleonics 16, No. 1: 88-90. 1958.

2. Melcher, James Russell and Murphy, Glenn. Electromagnetic field analogy for neutron diffusion theory. U. S. Atomic Energy Commission Report ISC-1136 (Ames Lab., Ames, Iowa). 1958.

3. Mossop, I. A. and McGhee J. Use of analogue wax model methods for reactor calculations, Second United Nations International Conference on the Peaceful Uses of Atomic Energy Proceedings 16: P/17 736-741. 1958.

4. Murphy, Glenn. Similitude in engineering. 2nd ed. New York, New York, Roland Press. 1950.

5. Corey, V. B., Green, J. H., and Frederick, C. L. Space simulator. U. S. Atomic Energy Commission Report AECD-2298 (Division of Technical Information Extension, AEC). 1947.

6. Fieno, Daniel, Schneider, Harold, Spooner, Robert B. Lumped fuel parameters for two-group reactor calculations. Nucleonics 11, No. 8: 16-18. 1953.

7. Honeck, H. C. and Ott, D. G. Application of analog computing techniques to the solution of neutron-flux distribution problems. Chemical Engineering Progress Symposium Series 50, No. 12: 107-112. 1954.

8. Liebmann, G. Solution of some nuclear reactor problems by the resistance: network analogue method. I. Journal of Nuclear Energy 2: 213-225. 1956.

9. Liebmann, G. Solution of some nuclear reactor problems by the resistance: network analogue method. II. Journal of Nuclear Energy 5: 169-185. 1957.

10. Eaton, J. R. and Long, R. L. An electrical analogy of nuclear reactor neutron flux. Unpublished. Lafayette, Indiana, (Department of Nuclear Engineering), Purdue University. Circa 1962.

11. Analog computer use in the nuclear field. Nucleonics 15, No. 5: 88. 1957.

12. Bayly, J. G. and Pearce, R. M. Method of studying multi-region reactors with an analog computer. Nuclear Science and Engineering 2: 352-362. 1957.

13. Kelber, C. N., Just, L. C. and Morehouse, N. F., Jr. The solution of many region reactor kinetics problems on an analog computer. Nuclear Science and Engineering 11: 285-289. 1961.

14. George, Robert E. and Sesonske, Alexander. Simplified simulation of a boiling water reactor power plant. Nuclear Science and Engineering 6: 409-413. 1959.

15. McK. Hyder, H. R., editor. Progress in nuclear energy, Series II, Reactors, Vol II. Pugamon Press, New York. 1961.

16. Dettman, John W. Mathematical methods in physics and engineering. New York, New York, McGraw Hill. 1962.

17. Handbook of Chemistry and Physics. 34th ed. (19, p. 2193) Cleveland, Ohio, Chemical Rubber Publishing Co. 1952.

18. Fenwal Electronics Incorporated. Transistor manual: EMC-5. Farmingham, Massachusetts, author. Circa 1960.

19. Glasstone, Samual and Sesonske, Alexander. Nuclear reactor engineering. (21, p. 806) Princeton, New Jersey, D. Van Nostrand Co., Inc. 1963.

20. Nuclear Engr. Handbook. 1st ed. New York, New York, McGraw-Hill. 1958.

VI. ACKNOWLEDGMENTS

The author acknowledges with pleasure the generous assistance extended during the development of this thesis.

Technical support was provided entirely by the complimenting efforts of Drs. Glenn Murphy and Donald M. Roberts. The classroom instruction in similitude, suggestion of a thermal-electric model and an analytical review of this paper were given by Dr. Murphy. Dr. Roberts directed the research, aided in the design of the epoxy testing technique, provided advisory council on reactor physics and suggested refinements in the presentation.

Other committee members who have participated in this work are Dr. Percy H. Carr, Dr. Arthur W. Davis and Dr. Agust Valfells.

Typing of the manuscript was done by Mrs. Marjorie Robison and Mrs. Deanna Carlson.

The epoxy resin was gratuitously furnished by the Minnesota Mining and Manufacturing Company.

Finally, the financial assistance by relatives and friends and especially the personal forbearance of my family is appreciated.

To all the above the author offers his thanks.

VII. APPENDIX A: PART I-DATA

Table 10. Spheres (epoxy shipment no. 1)

Model number	Milivolt readings for r/R values of: 0.00	0.25	0.50	0.75	1.00
Sphere 1a	2.20	2.06	1.58	1.16	0.69
Sphere 1b	2.35	2.19	1.82	1.41	0.91
Sphere 2a	4.42	4.04	3.56	2.07	1.10
Sphere 2b	4.52	4.39	3.35	2.26	0.96
Sphere 3a	7.60	7.40	6.72	5.60	0.80
Sphere 3b	7.63	7.38	6.96	5.37	1.17

Table 11. Cylinders and sphere no. 2 (epoxy shipment no. 2)

Model number	Radial milivolt readings for r/R values of: 0.00	0.25	0.50	0.75	1.00
Cylinder 4a	7.24	6.78	6.62	4.22	1.08
Cylinder 4b	7.75	7.48	6.74	5.02	1.12
Cylinder 5a	3.20	2.94	2.68	1.70	1.07
Cylinder 5b	3.19	2.93	2.71	1.93	0.85
Sphere 2c	5.98	5.58	5.32	3.15	1.04
Sphere 2d	6.72	6.56	5.53	3.67	1.08

Table 12. Cylinders

Model number	Axial milivolt readings for h/H values of: 0.00	0.25	0.50	0.75	1.00
Cylinder 4a	7.24	6.90	6.52	4.06	1.02
Cylinder 4b	7.75	7.40	6.90	4.32	1.07
Cylinder 5a	3.20	2.88	2.66	1.60	0.93
Cylinder 5b	3.19	2.90	2.57	1.50	0.82

VIII. APPENDIX B: PART I-ERROR ANALYSIS

The primary source of error is believed to result from slight misplacement of the thermocouples and the inadvertant formation of air bubbles at the interface of the epoxy and the model wall.

Errors in the thermocouple placement were found to be $\pm$ 0.08 cm as determined by slicing and measuring the hardened castings. A thermocouple misplacement will subsequently introduce an error in temperature measurement which depends jointly upon the error in position and the spacial rate of change of the maximum temperature. While the theoretical distribution functions are known to vary somewhat with the shape of the reactor, their slopes are nearly equal. If the distribution function is assumed to be $\cos \frac{\pi r}{2R}$ the slope is given by

$$-\frac{\pi}{2R} \sin\frac{\pi r}{2R}$$

so that the error is:

$$\text{error} = \pm \frac{\pi \Delta r}{2R} \sin\frac{\pi r}{2R}$$

Since the bubbles occur on the edge of the casting, it is reasonable that they would have more effect in that region than at the center. It is difficult to deduce what the exact distribution function for this sort of error should be but a sin function will again be assumed. This assumption appears to be validated by the trend in the data which shows progressively more scatter toward the edges of the castings. The relative error induced by bubbles is estimated to be 6%. Therefore the

total error is given by

$$\text{error} = \pm \sin \frac{\pi r}{2R} \left((0.06)^2 + \frac{(0.08)^2}{2R} \right)^{\frac{1}{2}}$$

It is noticed that while the method requires the distribution curve to intersect zero at the boundaries of the model, there is yet some uncertainty as to where that zero point should lie relative to the center of the curve whereas the assumed error at the center is zero. The scheme of error analysis has, then, somewhat arbitrarily referenced the entire curve to the central region.

Table 13. Part I Error tabulations

Model number	Calculated errors for π_1, or π_4 values of: 0.00	0.25	0.50	0.75	1.00
Radial errors					
1	0.000	0.024	0.044	0.058	0.063
2	0.000	0.023	0.043	0.056	0.061
3	0.000	0.023	0.042	0.055	0.060
4	0.000	0.023	0.043	0.056	0.061
5	0.000	0.024	0.044	0.057	0.062
Axial errors					
4	0.000	0.023	0.043	0.056	0.061
5	0.000	0.024	0.044	0.058	0.063

Note: All errors in above table are $\pm$.

As a supplemental comment about the error analysis, it might be mentioned that the effect of varying the mixing time and thermocouple size were both tested experimentally. When two cylindrical models, exact in other respects, were filled with batches of epoxy which had been mixed for 5 and 90 seconds respectively, the difference in maximum temperature was only one part in 147.

When a thermocouple had its junction bead size increased by a factor of eight, it yielded a value which differed by only one part in 128 when compared to a normal thermocouple symmetrically located in the same casting. Consequently, neither of these effects were judged to be significant.

Approximately 2/3 of the data lie in the error limits so that the flags drawn on Graphs 1, 2, and 3 may be interpreted as having a value of about one standard deviation.

Axial heat loss through the thermocouple wires is also a potential source of error. With the control position in the middle sized sphere as an example, the axial heat loss per second for a pair of wires is given by:

$$\frac{dH}{dt} = \frac{2\,A\,K\,\Delta\theta}{\Delta L}$$

$$= \frac{(2)(0.000202)(0.161)(85.2)}{3.51}$$

$$= 0.00158 \text{ calories/second.}$$

If the effective time is five minutes the total heat loss is 0.47 calories.

It is estimated that the effective sphere of epoxy material has a diameter equal to the midspan separation distance of adjacent thermocouples. The error in the temperature measurement would be then

$$\Delta\theta \text{ error} = \frac{H}{(\text{volume})(\text{specific gravity})(\text{specific heat})}$$

$$= \frac{0.47}{(9.61)(1.30)(0.35)}$$

$$= 0.11 \text{ Centigrade degrees.}$$

This is only about one part in 782 of the measured value and is therefore judged to be insignificant.

IX. APPENDIX C: PART II-DIMENSIONAL SUPPLEMENT

The following set of fundamental dimensions are adopted:

Mass $\doteq$ M

Length $\doteq$ L

Time $\doteq$ T

Heat $\doteq$ H

Temperature $\doteq$ θ

Where the symbol $\doteq$ means "has the dimensions of". Note that H is treated independently of ML and T when no work is done by the system as explained on page 193 of reference four.

Considering the equation

$$D\nabla^2\phi + (k-1)\Sigma a\,\phi = \frac{\partial n}{\partial t}$$

D = neutron diffusivity constant $\doteq$ L

ϕ = neutron flux $\doteq$ $L^{-2}\,T^{-1}$

n = neutron density $\doteq$ L^{-3}

k = neutron multiplication factor (a numeric)

Σa = macroscopic neutron captive cross section $\doteq$ L^{-1}

t = time $\doteq$ T

Substitution shows that all terms in the above equation have the dimensions $L^{-3}\,T^{-1}$.

For the equation

$$\frac{K}{\rho c}\nabla^2\theta + \frac{S}{\rho c}\theta = \frac{\partial\theta}{\partial t}$$

the terms are defined

K = thermal conductivity $\doteq H L^{-1} T^{-1} \theta^{-1}$

c = specific heat $\doteq H M^{-1} \theta^{-1}$

ρ = mass density $\doteq M L^{-3}$

θ = temperature $\doteq \theta$

S = specific rate heat generation term $\doteq H L^{-3} T^{-1} \theta^{-1}$

t = time $\doteq T$

Each term in the above equation has the dimensions θT^{-1}. In the text material the substitution of $\rho c \partial\theta/\partial t = \partial Q/\partial t$ has been occasionally made where Q = the heat per unit volume.

The condition of steady state operation which has been assumed throughout Part II also required that both $\partial\phi/\partial t$ and $\partial\theta/\partial t$ be zero.

The dimensional constants n_1 and n_2 are seen to be:

$n_1 \doteq L^{-2} T^{-1} \theta^{-1}$

$n_2 \doteq$ a numeric